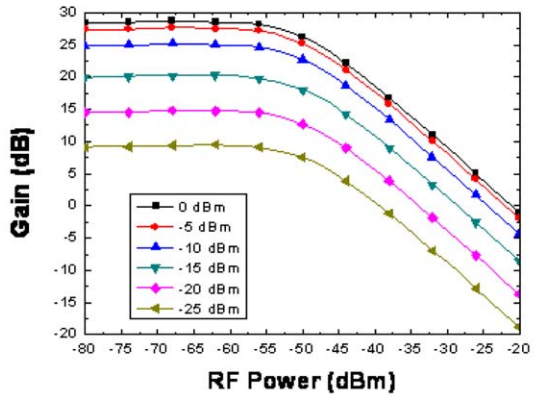

(a) Measured receiver voltage gain

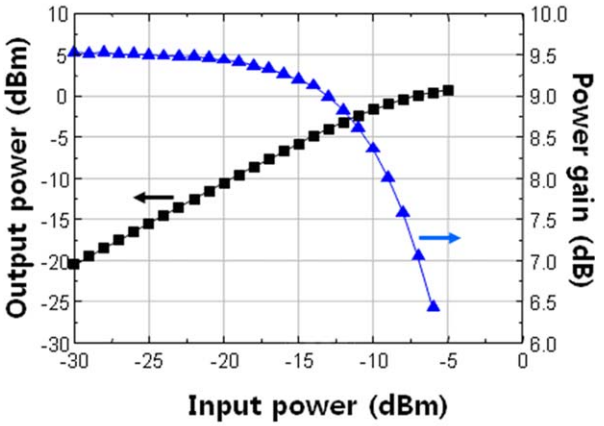

(b) Measured power gain and output P_{1dB}

Figure 8 Measured results (a) Measured receiver voltage gain and (b) Measured power gain and output P_{1dB}. [Color figure can be viewed in the online issue, which is available at wileyonlinelibrary.com]

TABLE 1 Performance Summary

Performance Parameters	Unit	Results
Radio frequency	MHz	402–405
Channels	–	10
Modulation	–	2-FSK
Data rate	Kbps	500
SNR	dB	17.0
Tx output	dBm	−2.8
Rx sensitivity	dBm	−85.0
Supply voltage	V	1.8
Power consumption	mW	22.0

5. CONCLUSION

A CMOS transceiver for ICTS is designed and fabricated. For low power consumption of the transceiver, the complex filter is adopted for image rejection and the PLL synthesizer is designed by digital logic circuits. Given these performance capabilities the 400 MHz transceiver can be applied to the medical equipments that need the wireless remote control.

ACKNOWLEDGMENT

This work was sponsored by the Korea Ministry of Trade, Industry and Energy.

REFERENCES

1. A.W. Astrin, H.B. Li, and R. Kohno, Standardization for body area networks, IEICE Trans Commun E92-B (2009), 366–372.
2. A.A. Emira and E.S. Sinencio, A pseudo differential complex filter for bluetooth with frequency tuning, IEEE Trans Circuits Syst 50 (2003), 742–754.
3. P.D. Bradley, An ultra-low-power high performance medical implant communication system transceiver for implantable devices, In: Proceedings of IEEE Bio Medical Circuits and Systems Conference, Singapore, November 2004, pp. 158–162.
4. A. Tekin, M.R. Yuce, J. Shabani, and W. Liu, A low-power FSK modulator demodulator for an MICS Band Transceiver, In: Proceedings of IEEE Radio and Wireless Symposium, San Diego, CA, January 2006.
5. M.R. Nezhad-Ahmadi, G. Weale, A. El-Agha, D. Griesdorf, G. Tumbush, A. Hollinger, M. Matthey, H. Meiners, and S. Asgaran, A 2 mW 400 MHz RF transceiver SoC in 0.18 um CMOS technology for wireless medical applications, In: Proceedings of IEEE Radio Frequency Integrated Circuits Symposium, Long Beach, CA, June 2008, pp. 285–288.
6. N.J. Cho, J.S. Bae, and H.J. Yoo, A 10.8mW body channel communication MICS dual-band transceiver for a unified body sensor network controller, IEEE J Solid-State Circuits 44 (2009), 3459–3468.
7. K. Suzuki, M. Ugajin, and M. Harada, A 5th–order switched capacitor complex filter for low-IF narrow band wireless receivers, In: Proceedings of IEEE Radio Wireless Symposium 2010, January 2010, pp. 420–423.
8. W. Khalil, S. Shashidharan, T. Copani, S. Chakraborty, S. Kiaei, and B. Barkkaloglu, A 700-mA 405-MHz all-digital franctional-N frequency locked loop for ISM band applications, IEEE Trans Microwave Theory Tech 59 (2011), 1319–1326.

AN X-BAND EIGHT-SUBARRAY SMART ANTENNA SYSTEM FOR DIRECTION OF ARRIVAL ESTIMATION

Yau-Hwa Tseng[1], Ing-Jiunn Su[1], and Ruey-Bing Hwang[2]
[1] Department of Electrical and Electronic Engineering, Chung Cheng Institute of Technology National Defense University, Taoyuan County 33551, Taiwan
[2] Department of Electrical and Computer Engineering, National Chiao-Tung University 1001 Ta-Hsueh Road, Hsinchu, 30010, Taiwan; Corresponding author: raybeam@mail.nctu.edu.tw

Received 31 March 2014

ABSTRACT: *An X-Band eight-subarray smart antenna system has been developed in this article to demonstrate its capability of direction of arrival estimation for correlated arriving signals. The antenna array is composed of an eight-subarray antenna and eight-track of transceiver for quadrature baseband to RF up/down conversion. Multiple classification of signal (MUSIC) and modified MUSIC algorithm with spatial smoothing are used for high resolution angle of arrival (AoA) estimation. Measured results showed that the modified MUSIC algorithm with spatial smoothing is capable of estimating target AoA with average angle error of 1.14° when target arriving angles are varying from −30° to 30°. Accurate results of AoA estimation by simulation and measurement for stationary or dynamic targets has also been demonstrated to validate the feasibility of the proposed X-Band smart antenna system.* © 2014 Wiley Periodicals, Inc. Microwave Opt Technol Lett 56:2582–2587, 2014; View this article online at wileyonlinelibrary.com. DOI 10.1002/mop.28654

Key words: *smart antenna system; angle of arrival estimation; multiple classification of signal*

1. INTRODUCTION

Phased array antennas and array signal processing technique for estimating the wave number and angle of arrival (AoA) of

multiple incident plane waves has wide applications in the areas of radar, sonar, electronic surveillance, medical diagnosis, and wireless communications. Direction of arrival (DoA) estimation is important for the applications of smart antennas, because AoA of a mobile unit is usually required before steering the antenna main beam to the desired targets.

Various DoA estimation algorithms are available for smart antenna application, for example, Bartlet, Capon, Min-norm, MUSIC, and ESPRIT [1–5]. Among these algorithms, MUSIC is probably the most popular one for high resolution and accurate applications. However, in case that the arriving signals are statistically correlated which results in reduction of the rank of the covariance matrix, the angle resolution of MUSIC algorithm can be seriously degraded. Another consideration is that DoA estimation usually require the knowledge of the number of arriving signals to discriminate the eigenvalues corresponding to signals or noise [6, 7]. To meet the above requirements by dividing the antenna array into smaller subarrays, spatial smoothing technique could determine the target's AoA by removing the correlation between the incoming sources, if the number of incoming sources is less than the number of synthesized subarrays [8, 9]. Forward–Backward spatial smoothing DoA estimation is implemented in this article for implementation of an X-Band eight-subarray smart antenna system [10–13].

This article is organized as follows. Section 2 is to introduce the basic principle of eigen-space decomposition of the MUSIC DoA estimators. Formulation of the MUSIC DoA algorithm and its modified version using forward–backward spatial smoothing technique follows afterward. The simulation and measured results that compare the performance of AoA resolutions between these two algorithms are shown in Section 3. Section 4 is the conclusion, followed by acknowledgment.

2. DOA ESTIMATION

2.1. Music Algorithm

In the application of mobile communications, multiple incident signals to a base station are usually coded to be mutually uncorrelated over a specific time interval. In this case, the conventional MUSIC algorithm is suitable for determining the incident angles of the incoming plane waves [14]. As shown in Figure 1, a uniform linear array (ULA) system is used to determine the AoA of each plane wave incidents on the array with various incident angles. Assuming there are N narrowband signals incident from N different angles, and the received ULA is with M-element. The received signal vector $x(t)$ is represented as

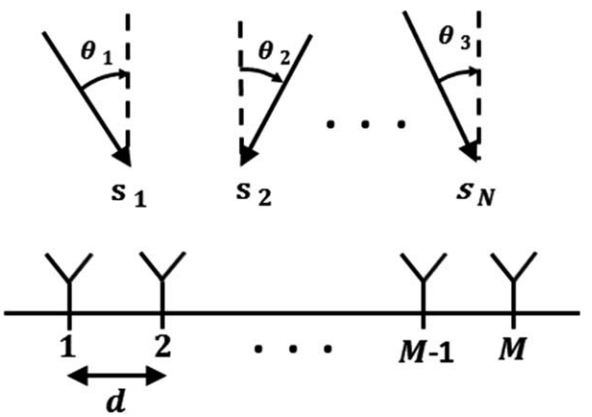

Figure 1 A uniform linear antenna array with M elements for determining AoA of the plane waves incident from various angles

$$\boldsymbol{x}(t) = [x_1(t) \quad x_2(t) \quad \cdots \quad x_M(t)]^T = \boldsymbol{A}\boldsymbol{s}(t) + \boldsymbol{n} \tag{1}$$

$$\boldsymbol{A} = [\boldsymbol{a}(\theta_1) \quad \boldsymbol{a}(\theta_2) \quad \ldots \quad \boldsymbol{a}(\theta_N)] \tag{1a}$$

$$\boldsymbol{s}(t) = [s_1(t) \quad s_2(t) \quad \cdots \quad s_N(t)]^T \tag{1b}$$

where $\boldsymbol{a}(\theta_i) = [e^{jk_0 d\sin\theta_i} \quad e^{jk_0 2d\sin\theta_i} \quad \ldots \quad e^{jk_0 Md\sin\theta_i}]^T$, and θ_i is the angle between direction of arriving signal i and the normal vector of ULA. The vector $\boldsymbol{a}(\theta_i)$ is the $M\times 1$ steering vector of array, $s(t)$ is the incident signal vector, n is the $M\times 1$ white Gaussian noise vector each with zero-mean and variance σ^2, k_0 is the frequency of incident signal, and d is distance between antenna elements. We define the correlation matrix of noisy signal vector $x(t)$ as:

$$\boldsymbol{R}_{xx} = E[\boldsymbol{x}(t)\boldsymbol{x}^H(t)] = \boldsymbol{A}E[\boldsymbol{s}(t)\boldsymbol{s}^H(t)]A^H + E[\boldsymbol{n}\boldsymbol{n}^H] \tag{2}$$

Assume that $s_1(t), s_2(t), \ldots, s_N(t)$ are uncorrelated signals, then the correlation matrix of received signal vector is $\boldsymbol{R}_{ss} = E[\boldsymbol{s}(t)\boldsymbol{s}^H(t)]$ with nonzero diagonal entries which are the received power of arriving signals. Therefore $\boldsymbol{R}_{ss}$ is a nonsingular matrix.

$$\begin{aligned} \boldsymbol{R}_{xx} &= \boldsymbol{A}E[\boldsymbol{s}(t)\boldsymbol{s}^H(t)]A^H + E[\boldsymbol{n}\boldsymbol{n}^H] \\ &= \boldsymbol{A}\boldsymbol{R}_{ss}A^H + \sigma^2\boldsymbol{I} \end{aligned} \tag{3a}$$

$$|\boldsymbol{R}_{xx} - \lambda_i\boldsymbol{I}| = 0, (\boldsymbol{R}_{xx} - \lambda_i\boldsymbol{I})\boldsymbol{v}_i = 0 \tag{3b}$$

If λ_i's are eigenvalues of $\boldsymbol{R}_{xx}$, $\lambda_1 > \lambda_2 > \ldots > \lambda_M$; and v_i is the corresponding eigenvector $i = 1, 2, \ldots, M$. For $M > N$, and $i = N + 1, N + 2, \ldots, M$, these eigenvalues are the received noise power, that is, $\lambda_i \cong \sigma^2$, so the corresponding eigenvectors v_i $i = N + 1, N + 2, \ldots, M$ construct a noise vector space. So, $(\boldsymbol{R}_{xx} - \lambda_i\boldsymbol{I})\boldsymbol{v}_i \approx \boldsymbol{A}\boldsymbol{R}_{ss}\boldsymbol{A}^H\boldsymbol{v}_i = 0$. As R_{ss} is a nonsingular matrix, then the array steering matrix $\boldsymbol{A}$ is orthogonal to v_i, when $i = N + 1, N + 2, \ldots, M$, that is, the array steering matrix is orthogonal to the noise subspace. Let matrix $V = [v_{N+1} \quad v_{N+2} \quad \ldots \quad v_M]$, and $P(\theta)$ be the spatial spectrum defined as:

$$P(\theta) = \frac{\boldsymbol{a}^H(\theta)\boldsymbol{a}(\theta)}{\boldsymbol{a}^H(\theta)VV^H\boldsymbol{a}(\theta)} \tag{4}$$

Thus the MUSIC algorithm for DoA estimation can be realized by searching the θ-values which peak the spatial spectrum $P(\theta)$.

2.2. Modified Music Algorithm with Spatial Smoothing

The above MUSIC algorithm is applicable if the incoming signals are mutually uncorrelated such that the correlation matrix $\boldsymbol{R}_{ss}$ satisfies full rank conditions for eigen-space decomposition. However, in a highly correlated channel environment, for example, active radars encounter multipath reflections when radio wave propagates, the correlation of incoming signals may severely degrade the DoA performance if only conventional MUSIC is used [15]. The idea of spatial smoothing proposed is a technique to recombine subset of the uniform arrays with forward and backward subarrays to resolve the singularity of the correlation matrix [12, 16–20]. The price paid is the reduced number of detectable users in the system.

Using the same definition of vectors as in the previous section, received vector of noisy signals can be written as:

$$\boldsymbol{x}(t) = [x_1(t) \quad x_2(t) \quad \cdots \quad x_M(t)]^T = \boldsymbol{A}\boldsymbol{s}(t) + \boldsymbol{n} \tag{5}$$

$$\boldsymbol{A}=[\,\boldsymbol{a}(\theta_1)\quad \boldsymbol{a}(\theta_2)\quad \ldots\quad \boldsymbol{a}(\theta_N)\,] \tag{5a}$$

$$\boldsymbol{s}(t)=[\,s_1(t)\quad s_2(t)\quad \cdots\quad s_N(t)\,]^T \tag{5b}$$

When the arriving signals are correlated, we can define the signals as $s_1(t)=\alpha_1 s_0(t)$, $s_2(t)=\alpha_2 s_0(t)$, ..., and $s_N(t)=\alpha_N s_0(t)$, assuming the signal power of $s_0(t)$ is normalized to one.

$$\boldsymbol{R}_{ss}=E[s(t)s^H(t)]=\alpha\alpha^H E[|s_0(t)|^2]=\alpha\alpha^H \tag{6}$$

$$\boldsymbol{s}(t)=[\,\alpha_1\quad \alpha_2\quad \cdots\quad \alpha_N\,]^T s_0(t)=\ s_0(t)\boldsymbol{\alpha} \tag{6a}$$

So $rank(\boldsymbol{R}_{ss})=1$, $\boldsymbol{R}_{ss}$ is no more an nonsingular matrix.

And the conventional MUSIC algorithm shall fail to distinguish the noise subspace and signal subspace. To solve the above problem, the spatial smoothing technique is to modify the conventional MUSIC algorithm as shown in Figure 2.

First, M element ULA is divided into L overlapping subarrays. Each subarray has $M_0=M-L+1$ elements. The received signal by lth subarray is denoted by $x_{Lf}(t)$.

$$\boldsymbol{x}_{l,f}(t)=[x_l, x_{l+1}, \ldots, x_{l+M_0-1}]=\boldsymbol{A}\boldsymbol{B}^{l-1}\boldsymbol{s}(t)+\boldsymbol{n}_l \tag{7}$$

$$\boldsymbol{A}=[\,\boldsymbol{a}(\theta_1)\quad \boldsymbol{a}(\theta_2)\quad \ldots\quad \boldsymbol{a}(\theta_N)\,] \tag{7a}$$

$$\boldsymbol{a}(\theta_i)=\left[\,e^{jk_o d\sin\theta_i}\quad e^{jk_o 2d\sin\theta_i}\quad \ldots\quad e^{jk_o M_0 d\sin\theta_i}\,\right]^T \tag{7b}$$

$$\boldsymbol{B}=\mathrm{diag}[a_{\theta_1}, a_{\theta_2}, \cdots a_{\theta_N}],\ \ a_{\theta_N}=e^{-jk_0 d\sin\theta_N} \tag{7c}$$

Where $\boldsymbol{A}$ represents the steering matrix of the array and $\boldsymbol{B}$ describes the phase relationship between subarrays. However, we should notice that the rank of $\boldsymbol{A}$ and $\boldsymbol{B}$ are dependent on the number of elements in subarray, not in the original ULA. The correlation matrix of lth subarray is given by:

$$\begin{aligned}\boldsymbol{R}_{l,f}&=E[\boldsymbol{x}_{l,f}(t)\boldsymbol{x}_{l,f}{}^H(t)]\\&=\boldsymbol{A}\boldsymbol{B}^{l-1}E[\boldsymbol{s}(t)\boldsymbol{s}^H(t)](\boldsymbol{B}^{l-1})^H\boldsymbol{A}^H+E[\boldsymbol{n}\boldsymbol{n}^H]\\&=\boldsymbol{A}\boldsymbol{B}^{l-1}\boldsymbol{R}_{ss}(\boldsymbol{B}^{l-1})^H\boldsymbol{A}^H+\sigma^2\boldsymbol{I}\end{aligned} \tag{8}$$

Here we define L-times spatial smooth covariance matrix as:

$$\boldsymbol{R}^f=\frac{1}{L}\sum_{l=1}^{L}\boldsymbol{R}_{l,f}=\boldsymbol{A}\boldsymbol{R}_{ss}{}^f\boldsymbol{A}^H+\sigma^2\boldsymbol{I} \tag{9}$$

$$\boldsymbol{R}_{ss}{}^f=\frac{1}{L}\sum_{l=1}^{L}\boldsymbol{B}^{l-1}\boldsymbol{R}_{ss}(\boldsymbol{B}^{l-1})^H \tag{9a}$$

The matrix $\boldsymbol{R}^f$ has the same form with $\boldsymbol{R}_{ss}$ in the conventional MUSIC algorithm, so it is necessary to inspect the rank of $\boldsymbol{R}^f$. Here,

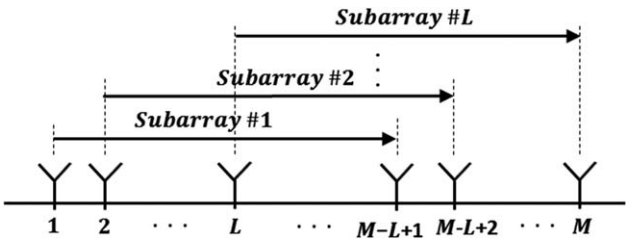

Figure 2 A uniform linear antenna array with M elements for determining AoA of the plane waves incident from various angles

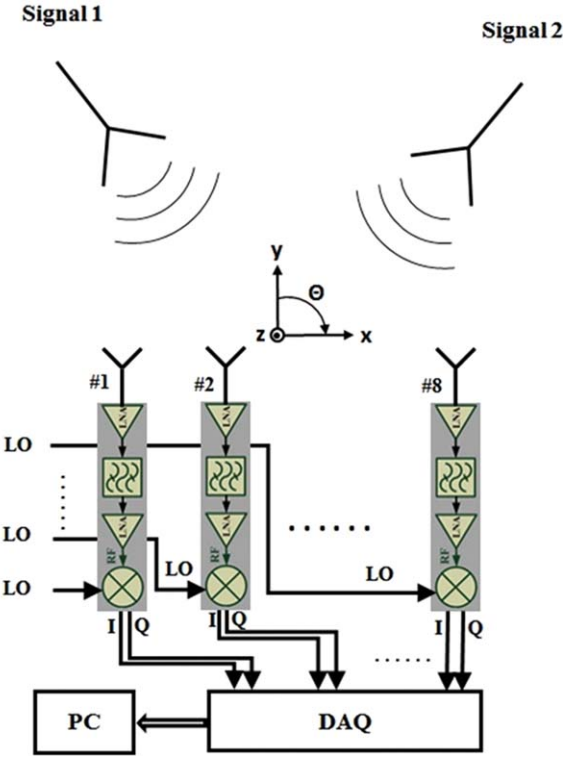

Figure 3 System architecture of an eight-subarray smart antenna. [Color figure can be viewed in the online issue, which is available at wileyonlinelibrary.com]

$$\boldsymbol{R}_{ss}{}^f=\frac{1}{L}\sum_{l=1}^{L}\boldsymbol{B}^{l-1}\boldsymbol{R}_{ss}(\boldsymbol{B}^{l-1})^H=\frac{1}{L}\boldsymbol{C}\boldsymbol{C}^H \tag{9b}$$

Where $\boldsymbol{C}$ is a $K\times L$ matrix given as follows,

$$\begin{aligned}\boldsymbol{C}&=\left[\,\boldsymbol{\alpha}\quad \boldsymbol{B}\boldsymbol{\alpha}\quad \boldsymbol{B}^2\boldsymbol{\alpha}\quad \boldsymbol{B}^{l-1}\boldsymbol{\alpha}\,\right]\\&=\mathrm{diag}[\,\alpha_1,\alpha_2,\quad \cdots\quad \alpha_N\,]\begin{bmatrix}1 & a_{\theta_1} & \cdots & a_{\theta_1}^{L-1}\\1 & a_{\theta_2} & \cdots & a_{\theta_2}^{L-1}\\ \vdots & \vdots & \ddots & \vdots\\1 & a_{\theta_N} & \cdots & a_{\theta_N}^{L-1}\end{bmatrix}\\&=\boldsymbol{D}\boldsymbol{V}\end{aligned} \tag{9c}$$

The rank of C is determined by matrix $\boldsymbol{V}$, as $\boldsymbol{D}$ is a nonsingular matrix. The matrix $\boldsymbol{V}$ is a vandermonde matrix with rank min (N,L). The above result is that the rank of $\boldsymbol{R}_{ss}^f$ is the same as that of $\boldsymbol{C}$ which is min (N,L). If $L > N$, that is the number of elements in subarray L is larger than the number N of the incoming signals, then rank($\boldsymbol{C}$) = N, and $\boldsymbol{R}_{ss}^f$ becomes a nonsingular matrix with rank N. The MUSIC algorithm modified with the above spatial smoothing technique becomes capable for predicting the incident angles among multiple correlated signals.

3. SIMULATION AND EXPERIMENTAL RESULTS

3.1. System Architecture of an Eight-Subarray Smart Antenna

In the experimental setup for DoA measurement is shown in Figure 3. The RF front-ends and local oscillator of the eight-

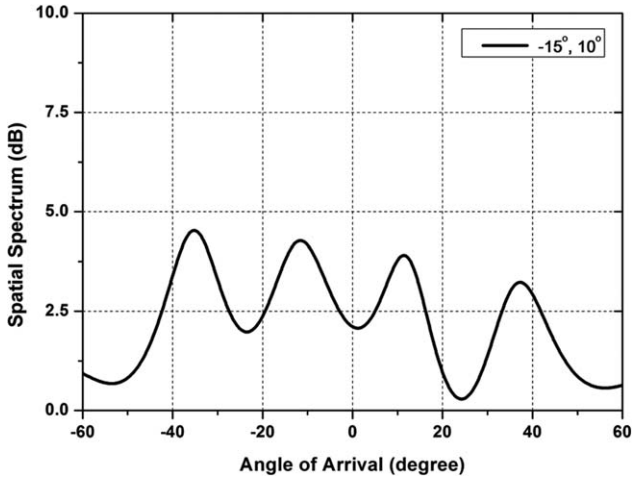

Figure 4 Simulation spatial spectrum using MUSIC only, with equal power coherent signals incident from −15° to 10°

element X-Band array elements are designed to operate at 9410 MHz. Subarrays are equally spaced by half-wavelength of the operating frequency. Low noise amplifier, band-pass filter, and down-conversion circuits are integrated into a module of the array system. The down-converted and low-passed IQ signals are digitally sampled by a data acquisition device controlled by a host PC computer. The sampled IQ data are collected and averaged to form an 8-by-8 correlation matrix for DoA estimation.

3.2. Simulation Results

For two coherent and equal power signals incident from −15°and 10° to the antenna array, the simulation results in Figures 4 and 5 are the estimated spatial spectra using MUSIC and modified MUSIC with spatial smoothing, respectively. The AoA angle, viz. direction of arrival, is defined positive if it is clockwise with respect to the broadside of the antenna array. The unpredictable result in Figure 4 shows that conventional MUSIC DoA algorithm fails to deal with correlated arriving signals. However, using the spatial smoothing MUSIC with length five of the subarray, a high resolution spatial spectrum results as depicted in Figure 5.

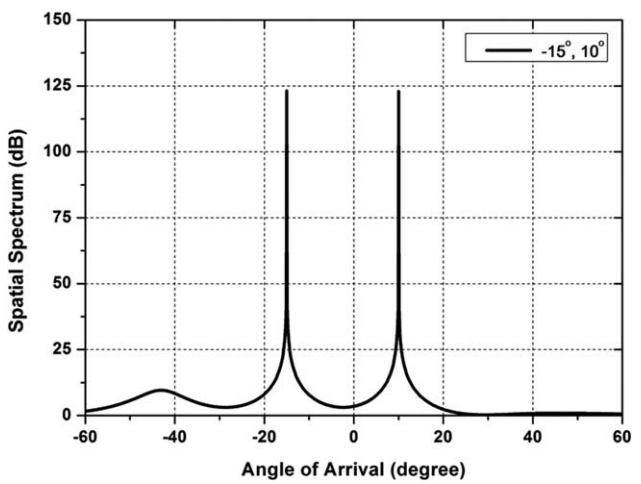

Figure 5 Simulation spatial spectrum using MUSIC with spatial smoothing with equal power coherent signals incident from −15° to 10°

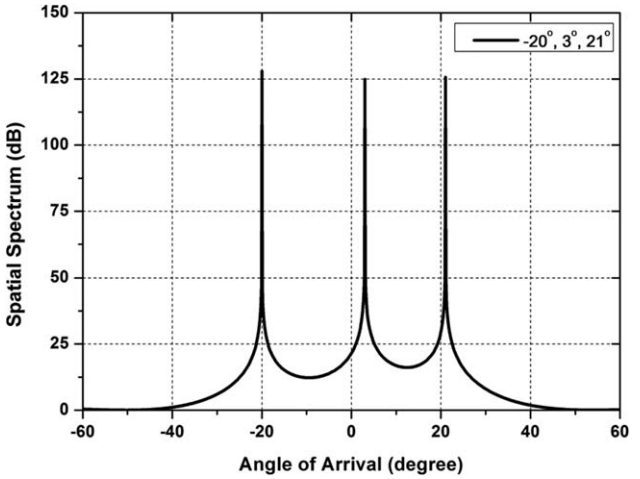

Figure 6 Simulated spatial spectrum using modified MUSIC with spatial smoothing technique, with three equal power coherent signals incoming from [−20°, 3°, and 21°] arriving angles

Now, if we increase the number of correlated targets in the system to three which are located at angles of ¯20°, +3°, and +21°. As given in Figure 6, the simulated spatial spectrum peaks exactly the same arriving angles as the incident waves.

3.3. Measured Results

Same as above, if two coherent and equal power signals incident from −15° and 10° to the antenna array, and use measured data for spatial smoothing MUSIC. The resultant spectrum is shown in Figure 7 which peaks at −14.5° and 10°, for two coherent and equal power signals incident from −15° and 10° to the system.

The measurement of a single stationary target in the anechoic chamber is shown in Figure 8. After each measurement, the target AoA incident angle was changed with a step size of 10° from −30° to 30°. The incident angles of waves with respect to the corresponding measured AoA are with angle errors between 0.2° and 2°. Figure 8 shows the measured spatial spectrum peaked at estimated DoA with respect to the incident AoA angles using MUSIC. The results show that for this case of

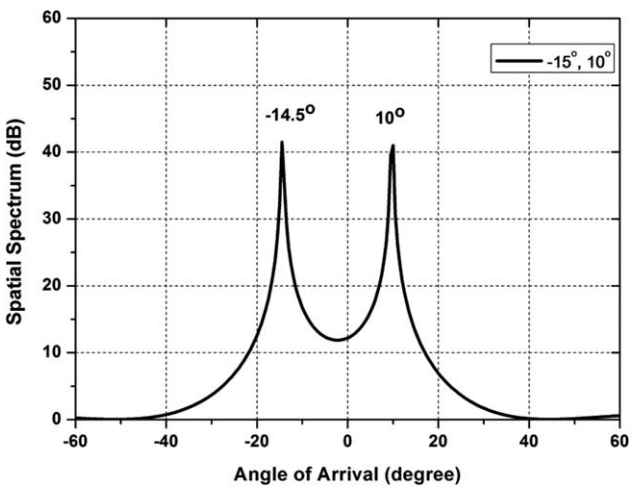

Figure 7 Measured spatial spectrum using spatial smoothing MUSIC with two coherent and equal power signals incident from −15° to 10°, respectively

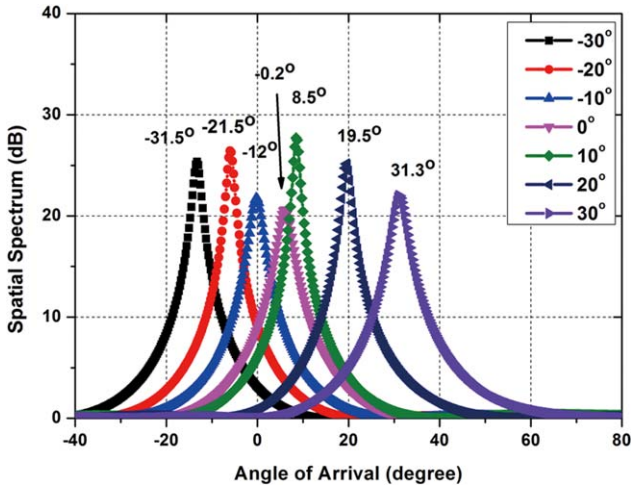

Figure 8 Measured spatial spectrum of a stationary target with the incident AoA angle changing from −30° to 30° (10° each step) in an anechoic chamber. [Color figure can be viewed in the online issue, which is available at wileyonlinelibrary.com]

single target only, conventional MUSIC works quiet well. The maximum measured angular error is 2° over all the seven measurements and the averaged angular error is 1.14°.

As mentioned above, the subarray length for the spatial smoothing MUSIC is chosen to be five, which means that the eight-element antenna array is capable constructing four subarray of length five. And the maximum number of correlated target in the system detectable using spatial smoothing MUSIC is also four. Now we increase the number of correlated targets in the system to three which are located at −20°, +3°, and +21°. As given in Figure 9, the measured spatial spectrum peaks at −20.5°, 0.5°, and 21.5° which result in 0.5°, 2.5°, and 0.5° angular errors, respectively.

3.4. Measuring DOA of a Single Moving Target

A measurement of AoA is setup with a target moving around the array antenna located as a central point. The distance between target and the array antenna is kept one meter in length. Measured results were given in Figure 10. The solid line in the figure was

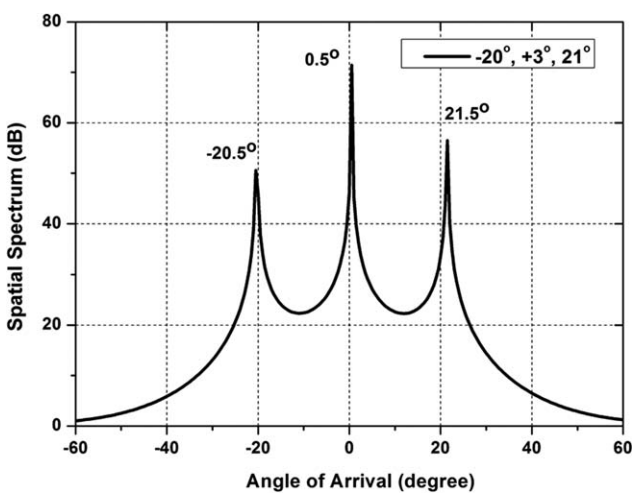

Figure 9 Measured spatial spectrum using spatial smoothing MUSIC for DoA with three equal power coherent signals incident from [−20°, 3°, 21°] AoA angles

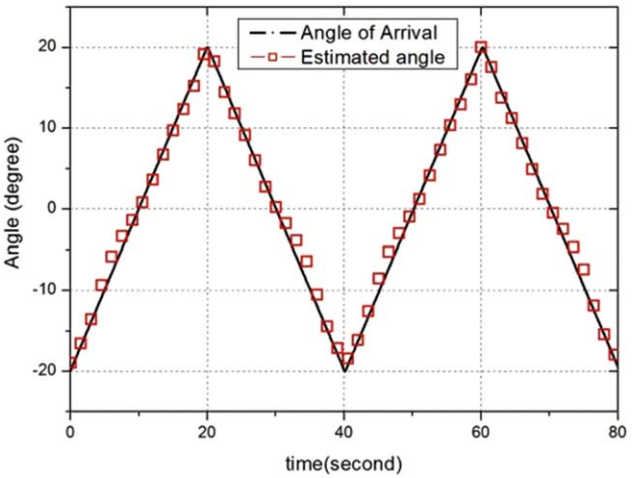

Figure 10 Estimated AoA and incident angle of a moving target with angular rate of two degrees per second. Measured data for modified MUSIC estimation algorithm were acquired from the eight-subarray X-Band array antenna. [Color figure can be viewed in the online issue, which is available at wileyonlinelibrary.com]

the target angle position and the DoA read-out angle in solid squares. The line of sight (a line connecting the moving target and the broadside of the array antenna) rate was set at two degrees per second and the range of angle scan is 40°. Apparently, with a dynamic DoA input to the system, the X-Band smart antenna is capable of tracking the moving target closely.

4. CONCLUSION

An eight-subarray X-Band smart antenna system has been successfully developed and demonstrated the capabilities of high resolution and accurate AoA estimation. MUSIC is suitable enough for uncorrelated targets estimation, however for correlated targets we used for better angle resolution. Measured results showed that the modified MUSIC algorithm could estimate stationary target with average angle error of 1.14° if target arriving angles range from −30° to 30°. Accurate tracking of a dynamically moving target around the array antenna system has also been demonstrated using modified MUSIC algorithm.

ACKNOWDEDGMENTS

The authors would like to thank the National Science Council, Taiwan, for financially supporting this research under Contract No. NSC 103-2623-E-009-004-D. The authors also appreciate CST Microwave Studio for supporting this research.

REFERENCES

1. A. Paulraj and T. Kailath, Eigenstructure methods for direction of arrival estimation in the presence of unknown noise fields, IEEE Trans Acoust Speech Signal Process 34 (1986), 13–20.
2. J.C. Liberti and T.S. Rappaport, Smart antennas for wireless communications: Is-95 and third generation CDMA applications, Prentice Hall PTR, Upper Saddle River, NJ, 1999.
3. L.C. Godara, Application of antenna arrays to mobile communications. Ii. Beam-forming and direction-of-arrival considerations, Proc IEEE 85 (1997), 1195–1245.
4. T.K. Sarkar, M.C. Wicks, M. Salazar-Palma, and R.J. Bonneau, Smart antennas, Vol. 170, Wiley, Hoboken, NJ, 2005.
5. F.B. Gross, Smart antennas for wireless communications: With MATLAB, McGraw-Hill, New York, 2005.
6. R.O. Schmidt, Multiple emitter location and signal parameter estimation, IEEE Trans Antennas Propag 34 (1986), 276–280.

7. G. Bienvenu and L. Kopp, Optimality of high resolution array processing using the eigensystem approach, IEEE Trans Acoust Speech Signal Process 31 (1983), 1235–1248.
8. H. Cox, R.M. Zeskind, and M.M. Owen, Robust adaptive beamforming, IEEE Trans Acoust Speech Signal Process 35 (1987), no. 10, 1365–1376.
9. B.D. Carlson, Covariance matrix estimation errors and diagonal loading in adaptive arrays, IEEE Trans Aerosp Electron Syst 24 (1988), 397–401.
10. S.U. Pillai and B.H. Kwon, Forward/backward spatial smoothing techniques for coherent signal identification, IEEE Trans Acoust Speech Signal Process 37 (1989), 8–15.
11. S.U. Pillai and B.H. Kwon, Performance analysis of music-type high resolution estimators for direction finding in correlated and coherent scenes, IEEE Trans Acoust Speech Signal Process 37 (1989), 1176–1189.
12. W. Xiao-guang and G. Tian-wen, Direction of arrival parametric estimation and simulation based on MATLAB, In: L. Jiang (Ed.), Proceedings of the 2011, International Conference on Informatics, Cybernetics, and Computer Engineering (ICCE 2011), 2011, Melbourne, Australia, Vol. 111, Springer, Berlin, 2012, pp. 147–156.
13. M.S. Amin, R. Ahmed Ur, M. Saabah Bin, K.I. Ahmed, and Z.R. Chowdhury, Estimation of direction of arrival (DOA) using real-time array signal processing, In: International Conference on Electrical and Computer Engineering, Dhaka, 2008, pp. 422–427.
14. R.T. Williams, S. Prasad, A.K. Mahalanabis and L.H. Sibul, An improved spatial smoothing technique for bearing estimation in a multipath environment, IEEE Trans Acoust Speech Signal Process 36 (1988), 425–432.
15. S.U. Pillai and B.H. Kwon, Forward/backward spatial smoothing techniques for coherent signal identification, IEEE Trans Acoust Speech Signal Process 37 (1989), 8–15.
16. S.U. Pillai and B.H. Kwon, Performance analysis of music-type high resolution estimators for direction finding in correlated and coherent scenes, IEEE Trans Acoust Speech Signal Process 37 (1989), 1176–1189.
17. X. Wu and T. Guo, Direction of arrival parametric estimation and simulation based on MATLAB, J Comput Inf Syst 6 (2010), 4723–4731.
18. T. Lobos, Z. Leonowicz, J. Rezmer, and P. Schegner, High-resolution spectrum-estimation methods for signal analysis in power systems, IEEE Trans Instrum Meas 55 (2006), 219–225.
19. T.-J. Shan, M. Wax, and T. Kailath, On spatial smoothing for direction-of-arrival estimation of coherent signals, IEEE Trans Acoust Speech Signal Process 33 (1985), 806–811.
20. S.U. Pillai and B.H. Kwon, Performance analysis of music-type high resolution estimators for direction finding in correlated and coherent scenes, IEEE Trans Acoust Speech Signal Process 37 (1989), 1176–1189.

A RECONFIGURABLE CIRCULAR PATCH ANTENNA WITH SWITCHABLE SLITS FOR POLARIZATION DIVERSITY

Mohamad N. Osman, Mohamad K. A. Rahim, Mohamad R. Hamid, Mohd F. M. Yusoff, and Huda A. Majid
Department of Communication Engineering, UTM-MIMOS Center of Excellence, Faculty of Electrical Engineering, Universiti Teknologi Malaysia, 81310, Johor Bahru., Malaysia; Corresponding author: mkamal@fke.utm.my

Received 2 April 2014

ABSTRACT: *This article proposes a novel circular patch antenna with polarization reconfigurability features. The antenna has a simple structure, which comprises of a radiating circular patch, embedded with two switches (PIN diode) and a pair of equal length slit on the top metal layer. By controlling the biased voltage of the PIN diodes, the polarization of the antenna can be reconfigured between three states; either linear polarization, right-hand or left-hand circular polarization. The details of the simulated and experimental results are presented and discussed. The proposed design has the potential application to improve channel reliability in a wireless communication system, especially in dealing with multipath-rich and limited space environment.* © 2014 Wiley Periodicals, Inc. Microwave Opt Technol Lett 56:2587–2590, 2014; View this article online at wileyonlinelibrary.com. DOI 10.1002/mop.28653

Key words: *circular patch antenna; slits perturbation; polarization reconfigurability; left/right hand circular polarization; linear polarization*

1. INTRODUCTION

In the multipath environment, the radio signal path regularly experiences the reflection duly from obstacles such as trees, cars, and buildings. This phenomenon becomes more challenging, especially in an indoor environment where a lot of reflections occur due to wall and furniture. Due to this phenomenon, the transmitted signal will be affected, and the signal reaching at the receiver will vary with different polarization and time. Consequently, at some proportion, receive signal may decreases, thus causing loss of effective communication.

Hence, one of the strategies to cater this problem is to have a single antenna with multifunctional feature; which is capable of offering various types of polarization modes. The antenna is able to transmit or receive with different polarizations which is linear polarization (LP) or circular polarization (CP) or between LP and CP. This polarization diversity type of antenna has received great attention recently due to its ability to expand the overall system capability such as the ability to reduce the multipath fading loss [1–3] and the realization of frequency reuse [4–6]. In addition, the polarization diversity antenna is also capable to improve performance of the system [7], such as for multiple-input-multiple-output (MIMO) systems [8].

Several antenna configurations with polarization diversity have been reported. The polarization diversity is successfully achieved by introducing the perturbation segments into the ground plane [4, 5] or radiating element [9–11]. In [12], the perturbation segment is created at both radiating elements as well as ground plane. Through this method, polarization diversity antenna with frequency agility is achieved. Besides the perturbation segment technique, the polarization reconfigurability design is proposed in [2, 13] through the development of tunable feeding network.

In this article, a circular patch antenna with the switched polarization capability is presented. Only two switches are required to obtain the polarization reconfigurability functions. Triple polarizations type can be obtained; LP, left-hand CP (LHCP) of right-hand CP (RHCP), by activating and deactivating the diodes. RF PIN diode Infineon BAR 50-02L is used as switches, located at a specific distance across the slit, thus controlling the length of the slit. This will enable the change of the current flow in the structure, which accordingly varies the polarization of the antenna. To activate the PIN diode, the biasing circuits are integrated with the structure. Details of the proposed design are described. The simulated and measured results are presented and the performances of the antenna are investigated. Full-wave simulations were performed using Computer Simulation Technology Microwave Studio.

2. DESIGN CONFIGURATION AND APPROACH

The geometry of the proposed polarization reconfigurable circular patch antenna is shown in Figure 1. The antenna is printed on a Taconic RF35 substrate with a height, h of 1.52 mm, permittivity of 3.54 and tangential loss of 0.0018. The size of the